Nano-based gas sensors

FABRICATION PROCESS

Chemical synthesis of WO_3 nanorods and integration on microelectronics devices for the realization of a gas sensor. Evaluation of the performance of the sensor under a controlled atmosphere.

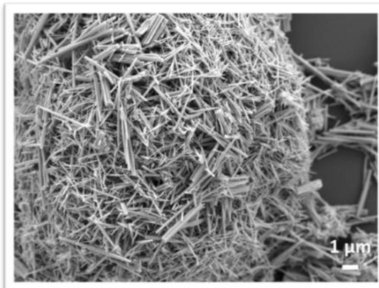

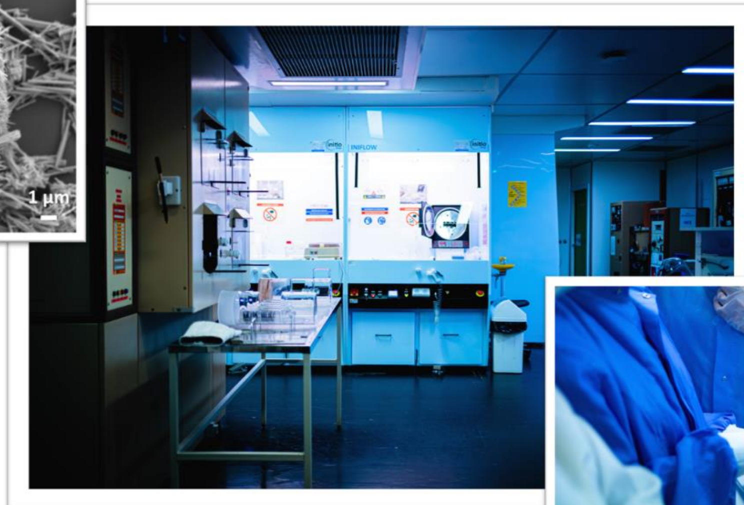

Practical works protocol

Summary

I. EVACUATION INSTRUCTION FOR TEACHERS 3
II. SAFETY INSTRUCTIONS 4
III. HANDLING INSTRUCTIONS 4
IV. CLEAN ROOM ENTRY PROCEDURE 5
V. INTRODUCTION 6
VI. PROCESS FOR CHIPS MANUFACTURING 7
A. MASKING OXIDATION 7
B. POLYSILICON DEPOSIT 8
C. POLYSILICON DOPING (n-type) 8
D. PHOTOLITHOGRAPHY N°1 : “POLYSILICON ETCHING” 9
E. SILICON DRY OXIDATION 11
F. PHOTOLITHOGRAPHY N° 2: « CONTACTS OPENING » 12
G. METALLIZATION 13
H. PHOTOLITHOGRAPHY N° 3 : " METAL ETCHING" 14
I. METAL ANNEALING 15
J. ASSEMBLY 15
VII. NANOPARTICLES SYNTHESIS 17
A. WO_3 NANORODS PREPARATION 17
VIII. NPs INTEGRATION BY DIELECTROPHORESIS 18
Material 18
Integration protocol 19
IX. MEASUREMENT UNDER CONTROLLED ATMOSPHERE 19
Bench test Initialization 19
Sensor characterization 20
X. ANNEXES 21
WO_3 Nanorods synthesis protocol 21
Temperature / voltage calibration curve of the aluminum resistance. 25
Protocol characterization of gas sensors (proposal) 26

I. EVACUATION INSTRUCTION FOR TEACHERS

REMINDER : Each teacher is responsible for the orderly and calm evacuation of all the students in his charge at the time of the disaster.

IN CLEAN ROOM N°1 :

- ⇨ Evacuate the students by the emergency exit which leads directly into the hall. Do not go through the airlock again; do not undress.

IN CLEAN ROOM N°2 :

- ⇨ Evacuate the students through the emergency exit leading to the electrical test room. Do not go through the airlock again; do not undress.

Gather all the students by the emergency exit that leads to the electrical test room.

Take a census.

Do not return to the premises without the advice of the firefighters or the director (or the technical manager present).

II. SAFETY INSTRUCTIONS

LOCATE **THE SAFETY EQUIPMENT**:

- emergency exits
- security showers
- fire extinguishers
- self-contained breathing equipment

WEAR PROTECTIVE GLASSES IS MANDATORY FOR:

- CHEMICAL CLEANING (RCA AND H_2SO_4-H_2O_2)

- ALL WET ETCHING

TRAINEES ARE **FORBIDDEN** TO TRANSPORT CHEMICALS FROM ONE WORKSTATION TO ANOTHER.

Keep in mind that:

- gloves are compulsory but they do not provide sufficient protection against high temperatures or corrosive products,
- some baths give off noxious vapors, normally drawn in by laminar flow hoods,
- overshoes sometimes make the floor very slippery.

III.HANDLING INSTRUCTIONS

- Throughout the duration of the process, the quality control of each step must be a permanent concern if we want to achieve a final component in working order, as well as a good performance on the whole. For this purpose, we will use in parallel with the "components" wafer, a control/test wafer (“witness”) which will characterize each step carried out.
- Warning: the wafers boxes must be opened by turning the cover clockwise.
- For handling a wafer with a tweezer :

- take advantage of the flat if the wafer is in the box

- pinch at least 5mm from the edge of the wafer to reduce the risk of breakage.

Any wafer coming out of a wet treatment must at the end undergo a rinsing with D.I. water and mechanical drying before being stored in its box.

- A good rinsing must include a change of tweezer, it is necessary to have a second one available and clean all tweezers.
- The tips of the pliers must not be wiped (neither on the gown, nor on paper), they must be rinsed with water and dried with nitrogen.
- The function of the gloves is to protect the components from contamination. Contamination of gloves should also be avoided. They are absolutely not an effective protection against acids.
- The plastic of the boxes cannot withstand temperatures above 250 ° C. In particular, cool down the wafers coming out from oven, for about 20 seconds in the open air.
- Paper is a source of contamination, make minimal use of it.

IV. CLEAN ROOM ENTRY PROCEDURE

- Leave street clothes and bags in the seminar room.

- Six lockers, lockable, can be used in the SAS for valuables.

- No more than 4 people in the airlock at the same time

Clean room entry:

Lab coat : white : permanent staff

blue: trainees

green: visitors.

overshoes : place the seam inside.

Do not put your foot in the clean part until you have put on your overshoes.

Mob caps : Provision in the wall dispenser.

gloves: Provision in the wall dispenser. 2 sizes available.

Mask surgery: brought by yourself.

Goggles: provision in the box.

Exit of clean room :

Lab coat/mob caps/goggles : place them in your personal box

Overshoes/gloves: throw them in dedicated trashes.

Recommendations:

- Be careful not to enter the SAS with muddy or wet dress shoes (use the doormat at the entrance of the AIME).

- Limit the number of objects and documents entering the Clean Room (**carbon pencil prohibited**).

V. INTRODUCTION

Gas sensors are equipment used in many fields (medicine, automotive industry, food industry, etc…). During the past years, the demand for methods of gas detection and measurement of their concentration has increased considerably. This interest is mainly due to environmental, safety or process control considerations, making gas sensors an important issue. In the field of gas detection, a distinction should be made between analyzers (analytical instruments) and chemical sensors. Chemical sensors have many advantages, including small footprint, low power consumption, low cost, and short response time. They can therefore be used for in-line process controls. Their main drawback is their selectivity. Indeed, gas mixture analysis often requires the use of several sensors sensitive to one or the other gas species. Semiconductor-type metal oxide sensors, such as the tungsten oxide WO_3 that we will be using, have the advantage of being relatively easily integrated into electronic circuits as we will see in this process.

GOALS :

The aim is to produce a gas sensor based on WO_3 nanoparticles (NPs) and then to evaluate it in a controlled gas atmosphere. The process then breaks down into 4 major steps:

- WO_3 NPs synthesis
- Fabrication of the microelectronic devices
- Integration of the active layer of NPs
- Electrical characterization of the sensor under controlled atmosphere

VI.PROCESS FOR CHIPS MANUFACTURING

The dies are composed of 4 elements:

- A buried heater (n-doped polysilicon)
- An Al resistance which can be used as a heater or a thermistor, located at the surface of the chips
- 2 interdigitated electrodes which will host the layer of nanoparticles and which will then become sensors sensitive to the gaseous environment.

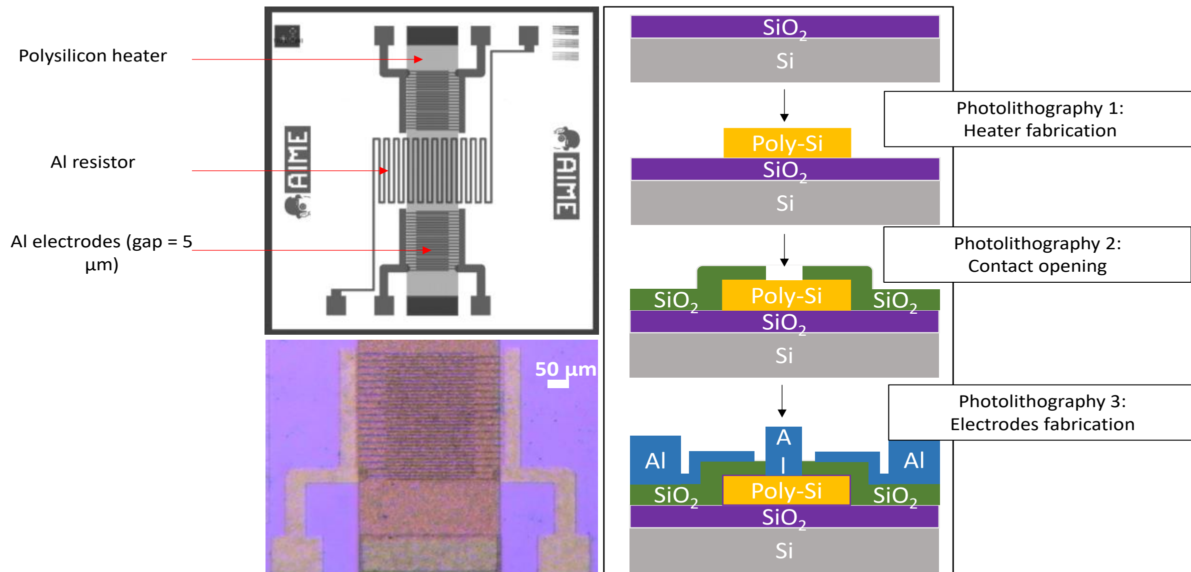

A. MASKING OXIDATION

The thickness of the masking oxide is around 4500 Å.

1- Cleaning before oxidation

- **Degreasing:** acetone, then water (hot)
- **chemical oxidation :** $H_2SO_4 + H_2O_2$ (1/1) 2 min, followed by DI water rinsing
- **SiO_2 etching:** dilute HF 30 s, followed by DI water rinsing
- **Drying:** spin dryer
- **cleaning/drying :** washer-dryer

2- Wet thermal oxidation: This operation is carried out in 5 steps in oven N°2-2

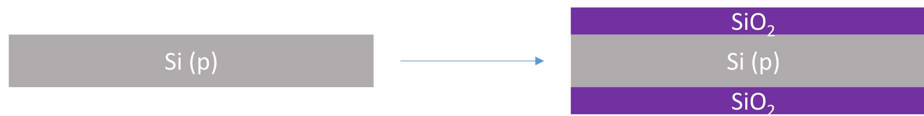

Temperature	Duration	Flow rate
⊂⊃ T = 800 to 1100°C	t = 25 min.	N_2 = 1 l/min.
⊂⊃ T = 1100 °C	t = 40 min.	H_2 = 2,7 l/min. O_2 = 1,5 l/min.
⊂⊃ T = 1100 °C	t = 30 min.	O_2 = 2,2 l/min.
⊂⊃ T = 1100 °C	t = 10 min.	Ar = 1,5 l/min.
⊂⊃ T = 1100 to 800°C	t = 60 min.	N_2 = 1 l/min.

B. POLYSILICON DEPOSIT

This is realized in LPCVD (Low Pressure Chemical Vapor Deposition) oven n°4-3.

Temperature	Duration	Flow rate	Pressure
T= 400°C to 585°C	t = 45 min.	N_2= 1 l/min.	p = 1 Torr
T= 585°C	t = 25 min.	SiH_4= 50 cc/min. PH_3= 2 cc/min.	p=250 mTorr
T= 585°C to 400°C	t = 4 x 2 min.	N_2= 1 l/min. : vent and vaccum cycles	p=1 Torr

C. POLYSILICON DOPING (n-type)

Doping of polysilicon is obtained by diffusion of phosphorus P impurities throughout its thickness.

1- Pre-deposit: This operation is performed in 3 steps in oven n°1-1

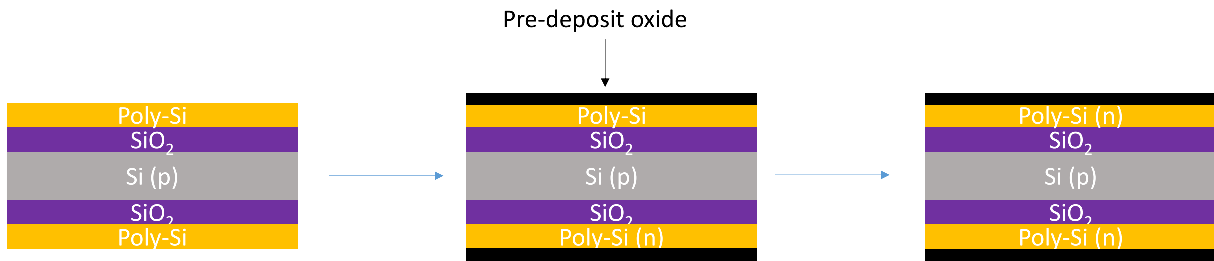

Conditions		
⊂⊃ put the "witness" wafer too		
Temperature	**Duration**	**Flow rate**
⊂⊃ 1050°C	5 min	N_2 = 2 l/min - O_2 = 0,1 l/min
⊂⊃ 1050°C	10 min	N_2 = 2 l/min - O_2 = 0,1 l/min – $POCl_3$ = 10 mg/min
⊂⊃ 1050°C	6 min	N_2 = 2 l/min - O_2 = 0,1 l/min

1- Dopant redistribution : performed in oven n°1-1:

Temperature	Duration	Flow rate
⊂⊃ 1100°C	7 min	N_2 = 1 l/min

2- Pre-deposit oxide etching :

⊂⊃ 1°) SiO_2 etching	Buffer HF : etching duration according to "witness" time
⊂⊃ 2°) Rinsing and drying	DI water then spin dryer

D. PHOTOLITHOGRAPHY N°1 : "POLYSILICON ETCHING"

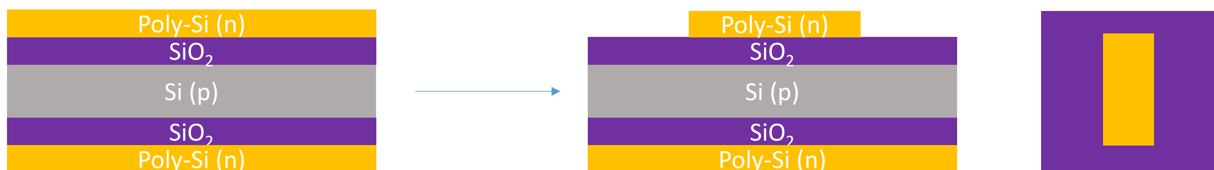

The manufactured doped polysilicon element will serve as a heating resistor buried under the gas sensors.

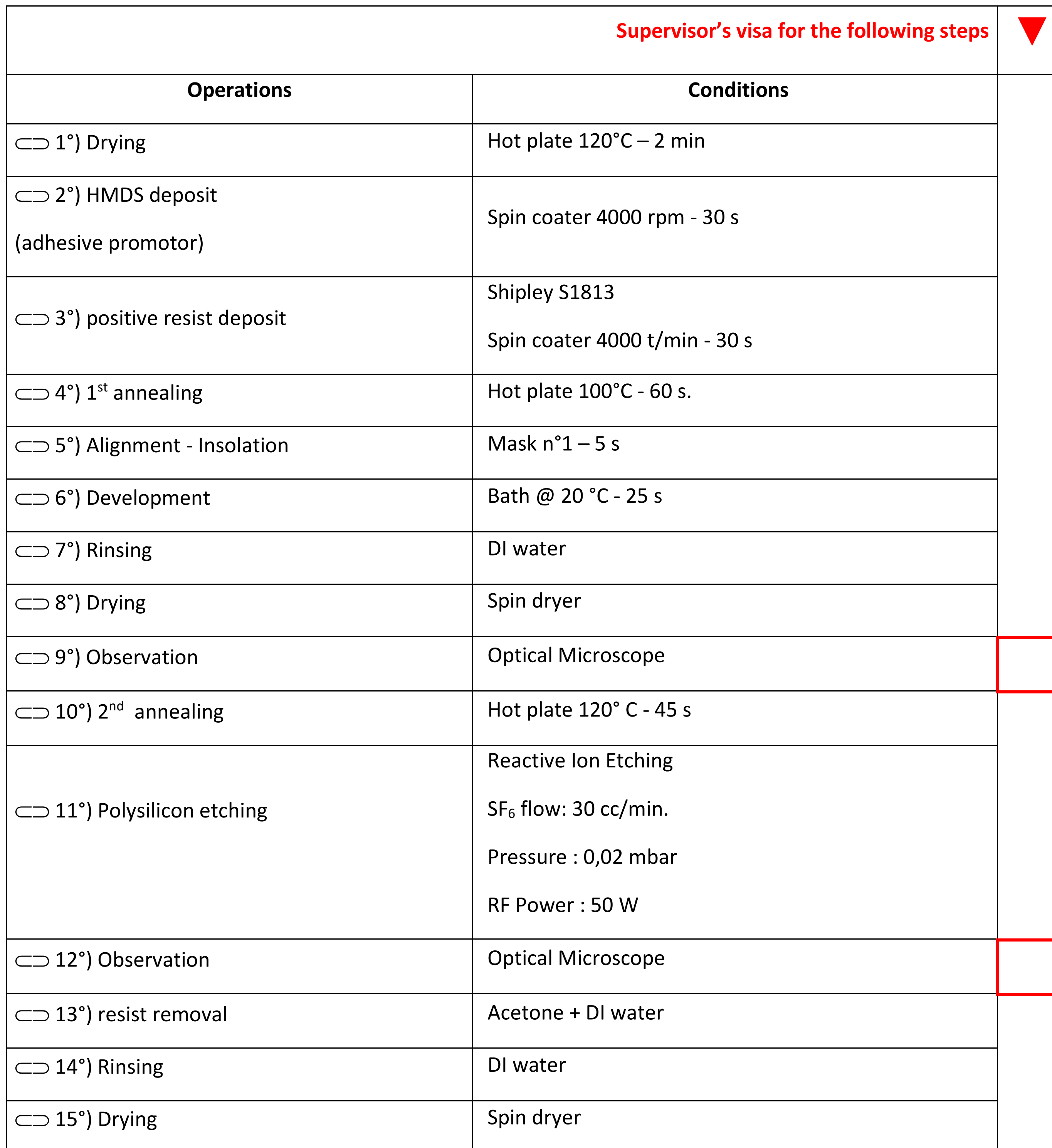

Supervisor's visa for the following steps		▼
Operations	**Conditions**	
⊂⊃ 1°) Drying	Hot plate 120°C – 2 min	
⊂⊃ 2°) HMDS deposit (adhesive promotor)	Spin coater 4000 rpm - 30 s	
⊂⊃ 3°) positive resist deposit	Shipley S1813 Spin coater 4000 t/min - 30 s	
⊂⊃ 4°) 1st annealing	Hot plate 100°C - 60 s.	
⊂⊃ 5°) Alignment - Insolation	Mask n°1 – 5 s	
⊂⊃ 6°) Development	Bath @ 20 °C - 25 s	
⊂⊃ 7°) Rinsing	DI water	
⊂⊃ 8°) Drying	Spin dryer	
⊂⊃ 9°) Observation	Optical Microscope	☐
⊂⊃ 10°) 2nd annealing	Hot plate 120° C - 45 s	
⊂⊃ 11°) Polysilicon etching	Reactive Ion Etching SF_6 flow: 30 cc/min. Pressure : 0,02 mbar RF Power : 50 W	
⊂⊃ 12°) Observation	Optical Microscope	☐
⊂⊃ 13°) resist removal	Acetone + DI water	
⊂⊃ 14°) Rinsing	DI water	
⊂⊃ 15°) Drying	Spin dryer	

Organic decontamination

Operations	Conditions
⊂⊃ 1°) cleaning	$H_2SO_4 + H_2O_2$ - 2 min
⊂⊃ 2°) Rinsing	DI water -2 min
⊂⊃ 3°) Drying	Spin dryer

E. SILICON DRY OXIDATION

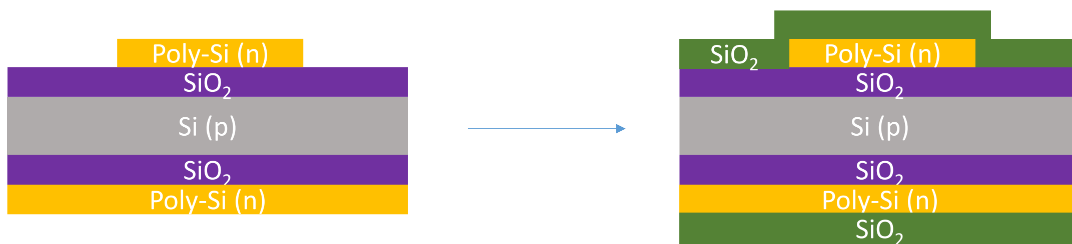

This dry thermal oxide growth takes place in oven N° 2-1:

Conditions		
⊂⊃ put the “witness” wafer too		
Temperature	**Duration**	**Flow rate**
⊂⊃ 1100°C	20 min	O_2 = 2 l/min
⊂⊃ 1100°C	10 min	Ar = 2 l/min

This step allows growing of a 300 nm-thick silicon oxide that will electrically insulate the conductive polysilicon from the aluminum tracks of the surface components.

F. PHOTOLITHOGRAPHY N° 2: « CONTACTS OPENING »

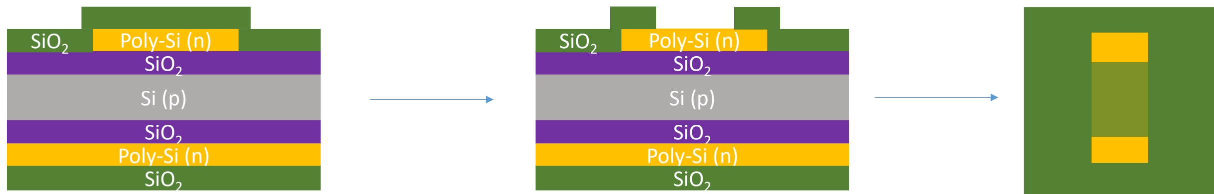

In order to electrically connect the polysilicon resistor, the dry oxide layer is opened at both ends, before the metallization step.

	Supervisor's visa for the following steps	▼
Operations	**Conditions**	
⊂⊃ 1°) Drying	Hot plate 120°C – 2 min	
⊂⊃ 2°) HMDS deposit (adhesive promotor)	Spin coater 4000 rpm - 30 s	
⊂⊃ 3°) resist deposit	Shipley S1813 Spin coater 4000 rpm - 30 s	
⊂⊃ 4°) 1st annealing	Hot plate 100°C – 60 s	
⊂⊃ 5°) Alignment - Insolation	Mask n°2 – 5 s	
⊂⊃ 6°) Development	Bath @ 20 °C - 35 s	
⊂⊃ 7°) Rinsing	DI water	
⊂⊃ 8°) Drying	Spin dryer	
⊂⊃ 9°) Observation	Optical microscope	☐
⊂⊃ 10°) 2nd annealing	Hot plate 120° C - 45 s	
⊂⊃ 11°) SiO_2 etching	Buffer HF : duration following "witness" wafer time*	
⊂⊃ 12°) Rinsing	DI water	
⊂⊃ 13°) Drying	Spin dryer	
⊂⊃ 14°) Observation	Optical microscope	☐

⊂⊃ 15°) Resist removal	Acetone
⊂⊃ 16°) Rinsing	DI water
⊂⊃ 17°) Drying	Spin dryer
⊂⊃ 18°) Give the "components" wafer to the technical staff for the metallization	

⊂⊃ *Polysilicon + oxide thickness measurement on “witness” wafer - **Operation n°1**

Test of the heater

Operations	Conditions
⊂⊃ 1°) Measure the polysilicon resistor	4 probes station

G. METALLIZATION

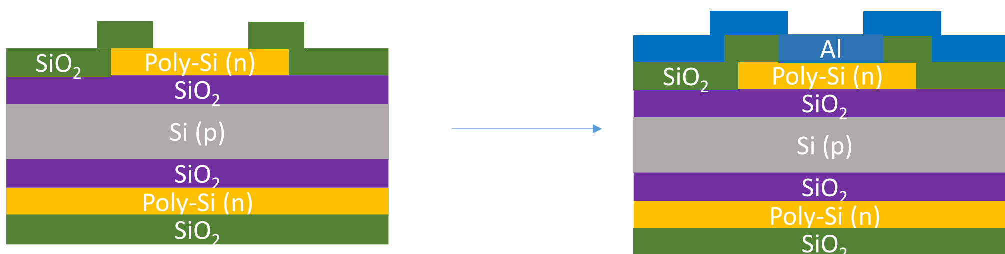

This operation consists of depositing on the component side a layer of 800 nm of aluminum.

Via RF sputtering :

⊂⊃ Deposit	Pressure before deposit = 10^{-7} mbar Pressure during deposit = 2.10^{-3} mbar RF power = 250 W Target-substrate distance = 75 mm Deposit duration = 10 min

H. PHOTOLITHOGRAPHY N° 3 : " METAL ETCHING"

This step aims to etch the aluminum and thus to define the electrodes of the sensors as well as the electrical contacts.

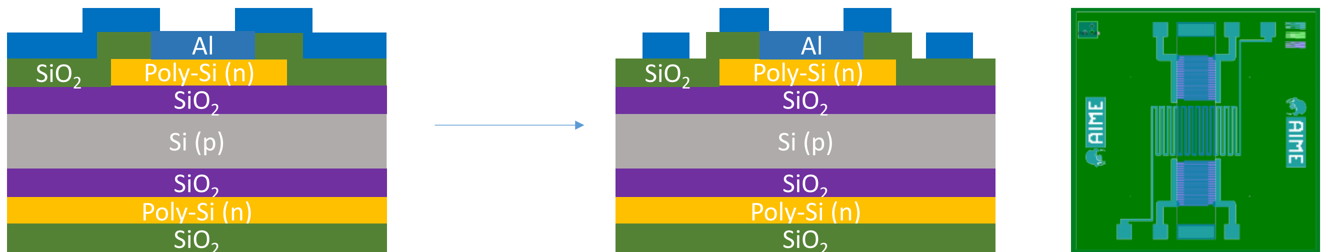

Operations	Conditions
⊂⊃ 0°) Homogenize aluminum etching bath	Place the Al etching bath in ultrasonic bath
⊂⊃ 1°) Drying	Hot plate (120°C) 5 min.
⊂⊃ 2°) Resist deposit	Shipley S1813 - Spin coater (4000 rpm, 30 s.)
⊂⊃ 3°) 1st annealing	Hot plate (100 °C) 60 s.
⊂⊃ 4°) Alignment - Insolation	Mask n°3 – 5 s
⊂⊃ 5°) Development	(20 °C), 30 s.
⊂⊃ 6°) Observation	Optical microscope
⊂⊃ 7°) 2nd annealing	Hot plate (120° C), 45 s.
⊂⊃ 8°) Al etching bath	Stop ultrasonic bath and remove Al etching bath
⊂⊃ 9°) Al etching	Etching bath (40vol. H_3PO_4 + 7vol. HNO_3 + 7vol. H_2O) final visual control + 30 s. additional etching
⊂⊃ 10°) Observation	Optical microscope
⊂⊃ 11°) Resist removal (2 sides)	acetone + DI water + drying with spin coater

I. METAL ANNEALING

⊂⊃ This step is performed in oven n°5-1:

Temperature	Temps	Flow rate
⊂⊃ T = 400 °C	t = 20 min.	N_2 + H_2 (5%)= 1 l/min.

⊂⊃ Measure the Al thickness on the components wafer using a profilometer.

J. ASSEMBLY

⊂⊃ DICING using a diamond dicing saw.

⊂⊃ SELECTION of best chips (component tracks not damaged) using optical microscope.

⊂⊃ ASSEMBLY on TO5 sockets: glue a square of glass with epoxy glue on the socket. Then stick the chip on its surface, still with epoxy glue. Polymerize the glue for the time required depending on the oven temperature (5 min at 110 ° C). Gently check the good mechanical strength of the assembly.

⊂⊃ WIRE-BONDING (Wedge bonding with Al-Si 5% wires, 25 µm diameter): connection of all components contacts pads to those of the base according to the following scheme:

.

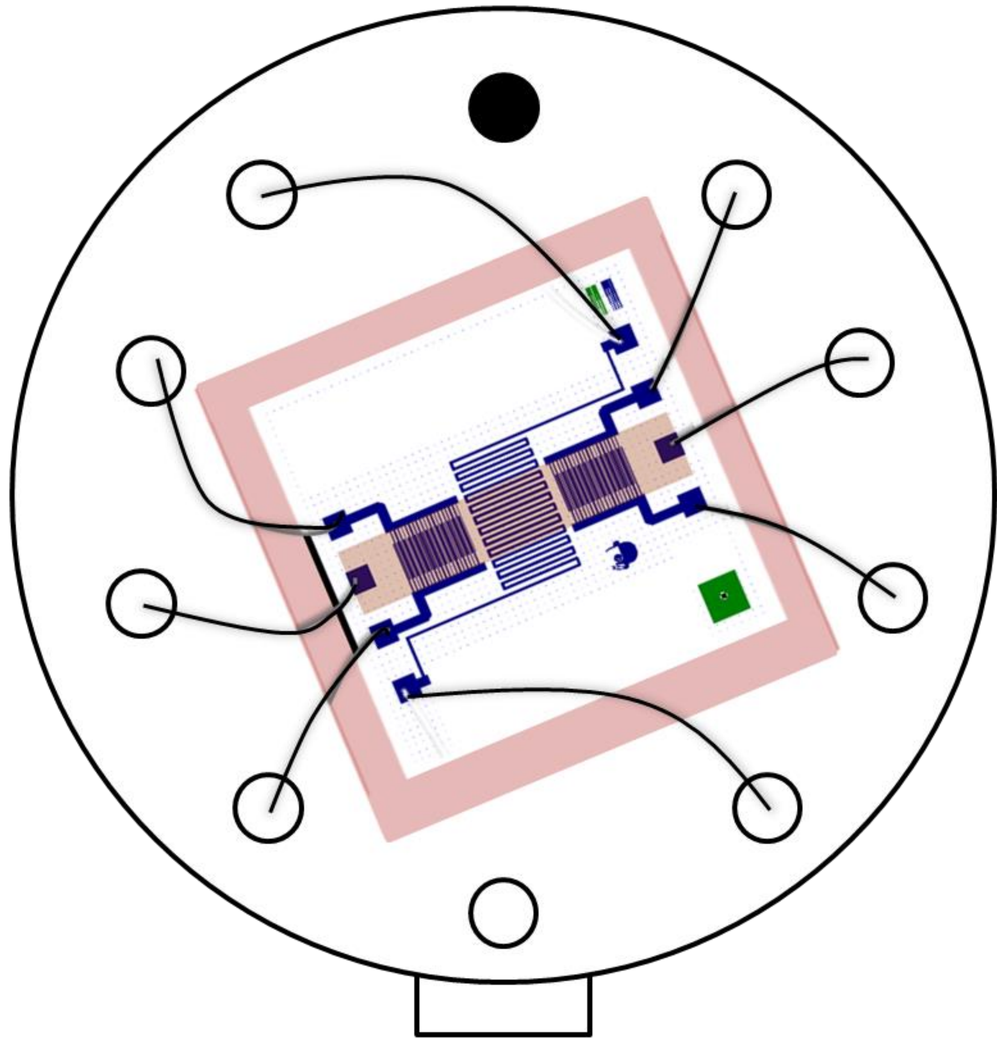

VII. NANOPARTICLES SYNTHESIS

The nanoparticles (NPs) synthesis follows a protocol which can be found in a scientific article given in appendix 1 *(Wang, J., Khoo, E., Lee, P. S., Ma, J. (2009) Journal of Physical Chemistry C, 113 (22), 9655–9658*). It is detailed below.

A. WO_3 NANORODS PREPARATION

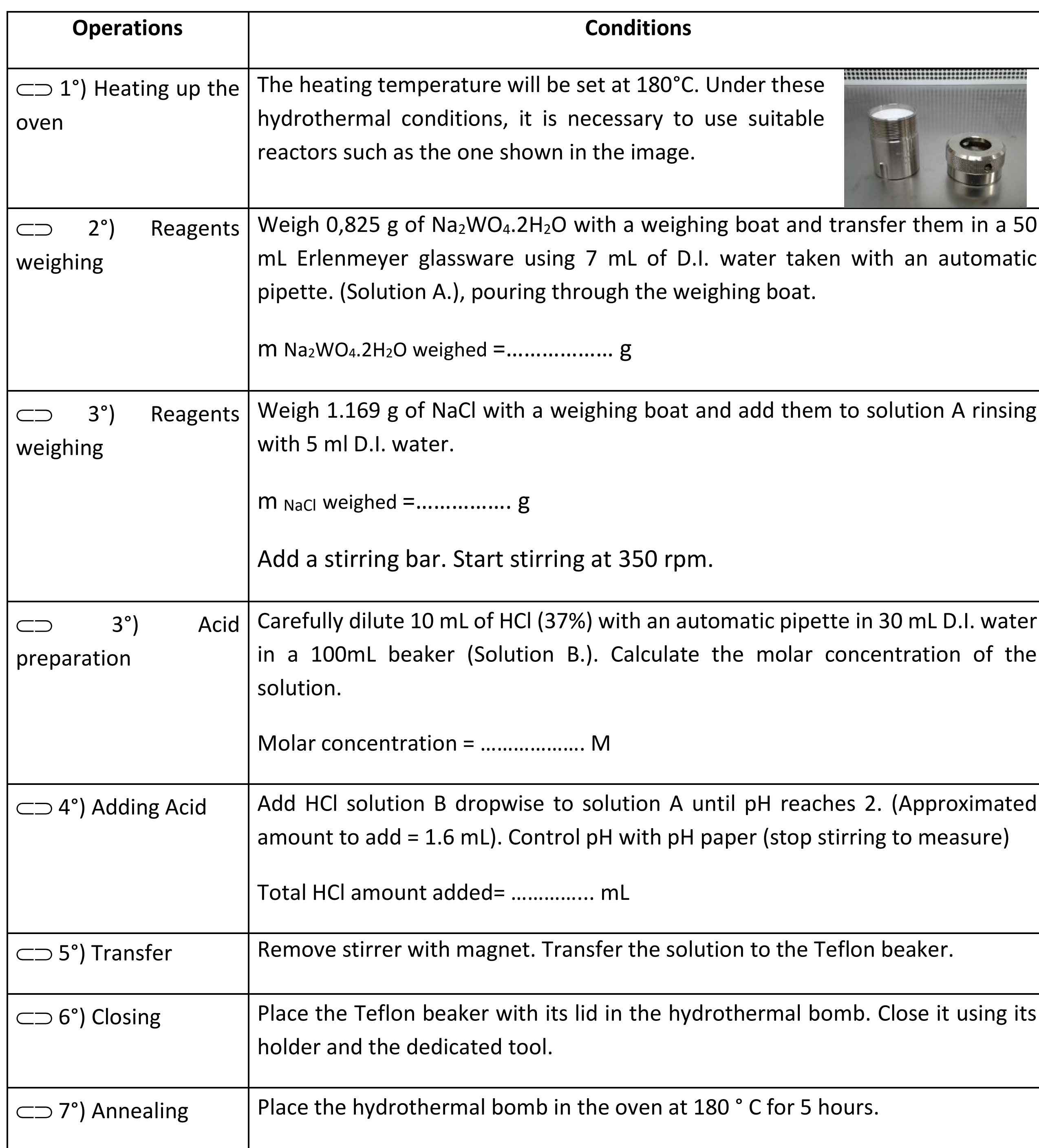

Operations	Conditions
⊂⊃ 1°) Heating up the oven	The heating temperature will be set at 180°C. Under these hydrothermal conditions, it is necessary to use suitable reactors such as the one shown in the image.
⊂⊃ 2°) Reagents weighing	Weigh 0,825 g of $Na_2WO_4.2H_2O$ with a weighing boat and transfer them in a 50 mL Erlenmeyer glassware using 7 mL of D.I. water taken with an automatic pipette. (Solution A.), pouring through the weighing boat. m $_{Na_2WO_4.2H_2O}$ weighed =................ g
⊂⊃ 3°) Reagents weighing	Weigh 1.169 g of NaCl with a weighing boat and add them to solution A rinsing with 5 ml D.I. water. m $_{NaCl}$ weighed =............... g Add a stirring bar. Start stirring at 350 rpm.
⊂⊃ 3°) Acid preparation	Carefully dilute 10 mL of HCl (37%) with an automatic pipette in 30 mL D.I. water in a 100mL beaker (Solution B.). Calculate the molar concentration of the solution. Molar concentration = ... M
⊂⊃ 4°) Adding Acid	Add HCl solution B dropwise to solution A until pH reaches 2. (Approximated amount to add = 1.6 mL). Control pH with pH paper (stop stirring to measure) Total HCl amount added= .... mL
⊂⊃ 5°) Transfer	Remove stirrer with magnet. Transfer the solution to the Teflon beaker.
⊂⊃ 6°) Closing	Place the Teflon beaker with its lid in the hydrothermal bomb. Close it using its holder and the dedicated tool.
⊂⊃ 7°) Annealing	Place the hydrothermal bomb in the oven at 180 ° C for 5 hours.

⊂⊃ 8°) Cooling	Carefully take the hydrothermal bomb out of the oven. Place it on a metal bench for 5 minutes then place it under the D.I. water tap until completely cool (about 15 min)
⊂⊃ 9°) Opening	Open the hydrothermal bomb and transfer its contents to a centrifuge tube. You can use 3 mL of D.I. water to rinse it well.
⊂⊃ 10°) Centrifugation	Collect the solution and pour it into a centrifuge tube. Weigh the tube and fill another tube with DI water, to match the masses. Place the tubes opposite in the centrifuge, then run at 10.000 rpm, for 5 minutes.
⊂⊃ 11°) Rinsing	Remove the supernatant and repeat once rinsing by centrifuging the nanorods with 3 mL of DI water.
⊂⊃ 12°) Storage	Transfer the nanorods to a pill container. Label your solution correctly.
⊂⊃ 13°) Cleaning and waste management	Clean the used glassware and dispose of the liquid contaminated waste in a Nano + Acid recovery container and the solid contaminated waste in the Nano solid waste recovery container.

VIII. NPs INTEGRATION BY DIELECTROPHORESIS

Material

- a voltage generator

- an oscilloscope

- connectors

- your solution containing NPs

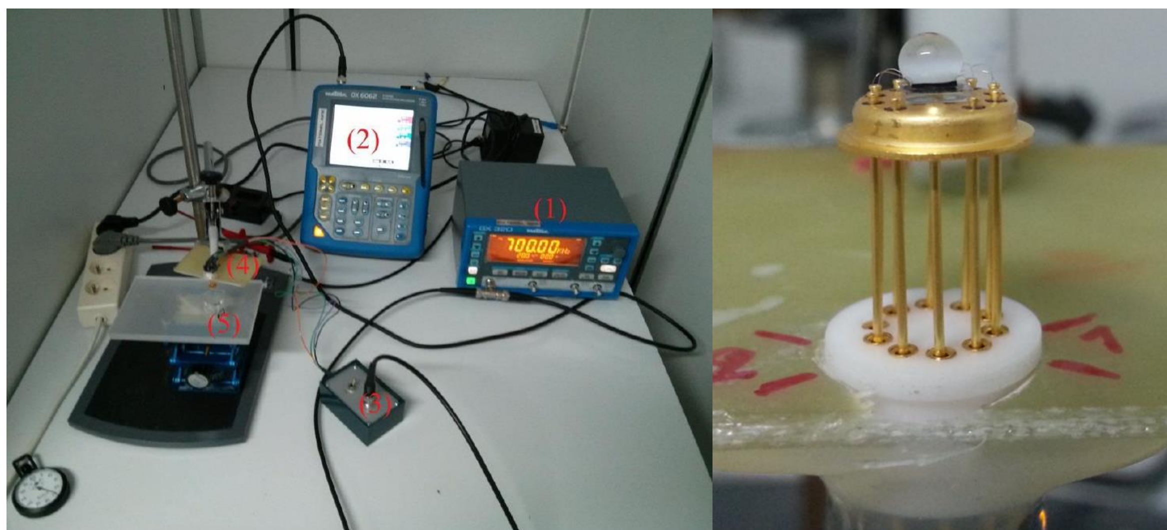

Integration protocol

A small amount of aqueous NPs solution is taken with a micropipette (around 10 mL) and a drop is deposited directly on the chip.

The interdigitated comb is then polarized with a sinusoidal voltage of frequency 100 kHz and amplitude 20 V_{pp}. This voltage is left for the duration of the integration.

After an integration time of ~ 120s, the excess water is mopped up with absorbent paper applied to the side of the chip, without damaging the bonding. At this time only, the polarization voltage of the inter-digit combs is cut.

The integrated sensor can then be observed under an optical microscope.

At this point the sensors are ready to be evaluated.

IX. MEASUREMENT UNDER CONTROLLED ATMOSPHERE

Bench test Initialization

You now have gas sensors ready for evaluation. We check the variation of their resistance in the presence of a specific gas at a given concentration.

The two gases we have are ammonia (NH_3) and ethanol (C_2H_6O), at a concentration of 0.1% in dry air (80% N_2 - 20% O_2).

To start the measurement:

• Connect your sample to the holder of the chamber, respecting the position of the tips. Remove the protective cap and close the chamber (screw).

• Open the gas valves located on the wall.

• Switch on the measuring devices.

• Start the Labview program and prepare the measurement by entering the work parameters:

o Check or modify the multimeter settings. The polarization voltage of the sensors must be 20V for all measurements.

o Choose the appropriate folder for recording data (you must first enter a file name to be able to browse the appropriate folder ... The file name can then be removed)

Sensor characterization

To modify the working temperature of the sensor, it is necessary to choose the applied voltage according to the calibration curve given in the appendix.

Warning! Do not change the voltage range until returning to zero voltage, otherwise it will induce a voltage peak that is fatal to the aluminum resistance. In addition, avoid sudden voltage variations so as not to induce significant thermal shocks in the resistance.

You can now define your own protocol for characterizing your sensors or choose the protocol provided in the appendix.

Once you have found the optimum operating temperature for your sensors, you can assess the influence of other parameters on their response (shape / size nanoparticles, deposit, applied voltage, etc.).

X. ANNEXES

WO_3 Nanorods synthesis protocol

J. Phys. Chem. C **2009,** *113,* 9655–9658 **9655**

Controlled Synthesis of WO_3 Nanorods and Their Electrochromic Properties in H_2SO_4 Electrolyte

Jinmin Wang, Eugene Khoo, Pooi See Lee,* and Jan Ma

School of Materials Science and Engineering, Nanyang Technological University, Singapore 639798, Singapore

Received: February 23, 2009; Revised Manuscript Received: April 23, 2009

Uniform crystalline WO_3 nanorods were synthesized by a lithium- or sulfate-free hydrothermal process with NaCl as a capping agent. It is found that variations in the pH and amount of capping agent have critical influence on the morphologies of the resultant WO_3 nanostructures. The electrochromic film comprised of the as-synthesized crystalline WO_3 nanorods exhibits a fast coloration/bleaching switching, coloration efficiency comparable to that of conventional amorphous WO_3 films, and a high H^+ ion-insertion ability in 0.5 mol/L H_2SO_4 solution without degradation.

1. Introduction

Tungsten oxide (WO_3) has attracted considerable attention due to its applications in electrochromic,[1−3] photocatalytic,[4] photoluminescent,[5] and gas sensing materials.[6] The generation of a color change that requires little or no additional input of power is the unique energy-saving or color-memory effect of electrochromic films, which is absent in other display devices such as liquid crystal displays (LCDs). As a well-known inorganic electrochromic material, WO_3 can display colorless and blue color by alternately applying positive and negative electrical voltages.[7] The electrochromic properties of WO_3 are of interest in energy-saving smart windows, antiglare mirrors, high contrast displays, and active camouflage.[8]

In the past decades, amorphous WO_3 was widely studied because of its fast electrochromic switching response[9−11] arising from its large specific surface area. However, amorphous WO_3 can only be used in lithium-based electrolytes due to its incompact structure and high dissolution rate in acidic electrolyte solutions. It is well-known that H^+ ions are smaller than Li^+, with an order of magnitude higher chemical diffusion coefficient than Li^+, resulting in a faster switching response in acidic electrolytes than that in lithium-based electrolytes.[12] Therefore, electrochromic materials that can endure acidic electrolytes without degradation should be developed. Crystalline WO_3 nanostructures with their much denser structures and small particle sizes are promising to be used as suitable electrochromic material in acidic electrolytes. Lee and Dillon et al.[12] have synthesized crystalline WO_3 nanoparticles by hot-wire chemical-vapor deposition and fabricated an electrochromic film by an electrophoresis deposition process at a high voltage of 300 V. The crystalline WO_3 nanoparticle films show comparable coloration efficiency and high stability compared to conventional amorphous WO_3 films. However, the actual coloration effect, contrast, and coloration/bleaching switching response were not reported. Recently, we have synthesized crystalline WO_3 nanorods, a type of one-dimensional (1D) nanostructures, from a simple solution route using NaCl as a capping agent and studied their electrochromic properties in a lithium-based electrolyte.[13]

In this report, we demonstrate the morphology-control approaches and establish the correlation between the solution reaction conditions and the resultant morphologies of WO_3 nanostructures. Besides, we present the electrochromic properties of the WO_3 nanostructured films carried out in an acidic electrolyte, which provides small and quickly inserted ions (H^+ ions).

2. Experimental Section

2.1. pH of the Precursor Solutions. WO_3 nanorods were synthesized using the recently reported hydrothermal process with NaCl as a capping agent.[13] $Na_2WO_4 \cdot 2H_2O$ (0.825 g, 0.0025 mol) was used as the tungsten source and dissolved into 19.0 mL of deionized H_2O. The pH value of Na_2WO_4 solution is 7.9 and a precipitate was formed when excess HCl was added into the precursor solution to reach a pH of 1.2 at room temperature. Thus, hydrothermal reactions were carried out for the precursors with pH 1.2−7.9. Since the suitable amount of capping agent NaCl has not been defined, we used 1.160 g (0.020 mol) of NaCl capping agent for the hydrothermal synthesis. To all of the precursors 1.169 g of NaCl was added.

2.2. Amount of Capping Agent NaCl. A series of weights of NaCl were examined to find the optimum amount of NaCl; 0.290 g (0.005 mol), 0.580 g (0.010 mol), 1.160 g (0.020 mol), and 2.320 g (0.040 mol) of NaCl were respectively added into Na_2WO_4 solution to obtain the precursor solutions. As comparison, a solution of Na_2WO_4 without NaCl (0 g of NaCl) was used as a reference precursor. All of the hydrothermal experiments were carried out at 180 °C for 24 h.

2.3. Preparation of Electrochromic Film. The electrochromic film was prepared using the as-synthesized WO_3 nanorods following the reported method.[13] Drop-assembly of the stable WO_3 suspension was carried out on a cleaned ITO glass and has been found to follow the aggregation−deposition mechanism.

2.4. Characterization. The phase of the product was identified by X-ray powder diffraction (XRD, Shimadzu), using Cu Kα ($\lambda = 0.154\ 06$ nm) radiation at 50 kV and 50 mA in a 2θ range from 10° to 80° at room temperature. The morphologies of the as-synthesized WO_3 nanorods and the nanorod-coated film were characterized by field-emission scanning electron microscopy (FESEM), using an accelerating voltage of 5 kV and beam current of ∼12 μA. Transmission electron microscopy (TEM) and high-resolution transmission electron microscopy (HRTEM) images and selected area electron diffraction (SAED) pattern of the WO_3 nanorods were obtained on a JEM-2010

* Author to whom correspondence should be addressed. Tel: 65-67906661. Fax: 65-67909081. E-mail: pslee@ntu.edu.sg.

10.1021/jp901650v CCC: $40.75 © 2009 American Chemical Society
Published on Web 05/12/2009

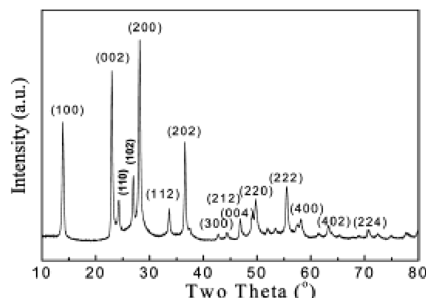

Figure 1. XRD pattern of the hydrothermal product.

microscope, using an accelerating voltage of 200 kV. Electrochromic properties of the as-synthesized WO_3 nanorods were measured by a two-electrode electrochemical cell with 0.5 mol/L H_2SO_4 aqueous solution as the electrolyte. The measurements were carried out by using the Autolab Potentiostat (PGSTAT302). The electrochromic film coated by WO_3 nanorods was vertically inserted into the electrolyte and acted as the working electrode; Pt wire was used as the counter electrode. In situ transmittance spectra were measured by UV−vis spectrophotometer (UV-2501 PC SHIMADZU) in standard cuvettes in the spectral region between 300 and 900 nm. In situ coloration/bleaching switching characteristics of the electrochromic film were recorded with an absorbance wavelength of 632.8 nm by alternately applying voltages of −1.0 and +1.0 V, respectively.

3. Results and Discussion

Figure 1 shows the XRD pattern of the as-synthesized WO_3 nanorods. All of the peaks can be well-indexed to the hexagonal phase of WO_3 (JCPDS 85-2460). The sharp peaks indicate the as-synthesized product was well-crystallized.

To determine the optimum reaction condition for the synthesis of uniform crystalline WO_3 nanorods, the influence of pH value and the amount of capping agent NaCl on the morphologies of the hydrothermal products was investigated. The pH value is the most critical parameter for the synthesis of one-dimensional WO_3 nanostructures. No precipitate was formed by hydrothermal treatment when only Na_2WO_4 solution was used as the precursor (pH 7.9, 0 g of NaCl). However, hydrothermal products can be obtained when the pH values of the precursors are 1.5−3.0 by adding HCl solution.

Figure 2 shows the FESEM images of the hydrothermal products synthesized at pH 1.2, 1.5, 1.8, 2.0, 2.5, and 3.0. It can be seen that the hydrothermal product synthesized at pH 2.0 consists of uniform nanorods (Figure 2d). However, the products are irregularly aggregated smaller-sized nanostructures (Figure 2a−c) and larger-sized microspheres (Figure 2e,f) at smaller pH values and larger pH values, respectively. This result can be explained by the well-known theory for crystal nucleation and growth.[14] The formation of WO_3 nanorods depends on the decomposition of H_2WO_4 formed by WO_4^{2-} ions and H^+ ions.[13] For the formation of H_2WO_4, H^+ ions served as one of the reactants. The acidity of the precursor and therefore the pH values affect the crystal growth of WO_3 nanorods. It is well-known that crystal growth comprises two major stages: nucleus formation and subsequent growth. Supersaturation is the driving force for nucleus formation, and the number of crystals increases with increasing supersaturation.[14] At a smaller pH value (a larger concentration of H^+ ions), a great deal of small WO_3 nuclei are quickly generated, due to the larger supersaturation of H_2WO_4, and then the supersaturation reaches a low level, which results in a slow subsequent growth. The formed small nuclei possess a large active specific surface area, so they are easily aggregated. As a result, dense and small nanostructures with a serious agglomeration are formed. At a larger pH value, less crystal nuclei are generated, because of the smaller supersaturation of H_2WO_4, which favors the subsequent growth. As a result, bigger particles are formed finally. An optimum pH value for the growth of WO_3 nanorods should lie in the middle pH range; this is found to be pH 2.0 according to our experimental results. The effects of pH on the morphologies of a variety of nanostructures have also been reported in the formation of WO_3 nanowires,[15] ZnO nanorods,[16] and $BaSO_4$ nanofibers.[17]

To assess the optimum amount of capping agent NaCl for the synthesis of WO_3 nanorods, hydrothermal reactions were carried out with NaCl amounts of 0, 0.290, 0.580, 1.160, and 2.320 g at pH 2.0, respectively. Figure 3 shows the FESEM images of the hydrothermal products (the FESEM image of the product synthesized with 1.160 g of NaCl is shown in Figure 2d). It can be seen that excess NaCl (2.320 g) results in a poor uniformity in the rodlike morphology of WO_3 nanostructures (Figure 3d). Lower amounts (0.290−1.160 g) of NaCl attained the uniform rodlike morphology of WO_3 nanostructures (Figures 2d and 3b,c). However, a serious agglomeration of nanorods occurred when no NaCl was used in the precursor; as a result, nanorod bundles with larger diameters were formed (Figure 3a).

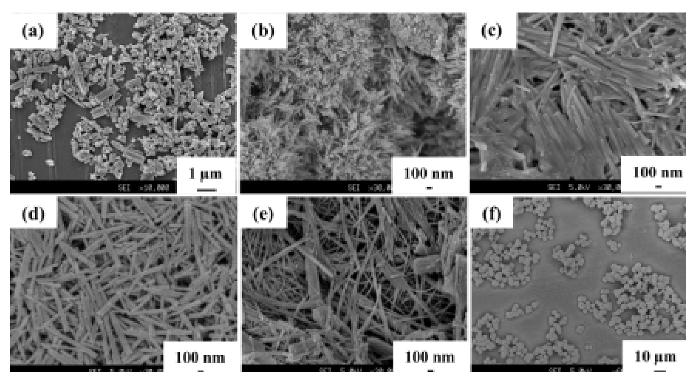

Figure 2. FESEM images of hydrothermal products synthesized at pH (a) 1.2, (b) 1.5, (c) 1.8, (d) 2.0, (e) 2.5, and (f) 3.0.

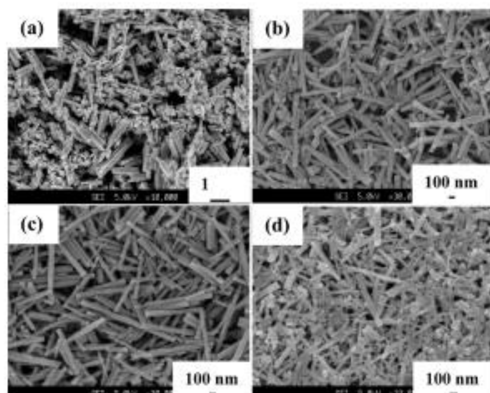

Figure 3. FESEM images of hydrothermal products synthesized with (a) 0 g, (b) 0.290 g, (c) 0.580 g, and (d) 2.320 g of NaCl.

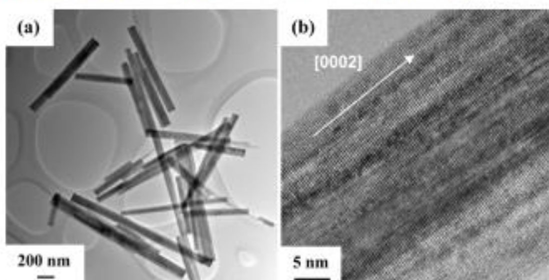

Figure 4. (a) TEM and (b) HRTEM images of the as-synthesized WO_3 nanorods.

Figure 4 shows the TEM and HRTEM images of the as-synthesized WO_3 nanorods. The lattice spacing of 0.38 nm corresponds to the *d*-spacing of (0002) planes, which indicates that the growth direction of the as-synthesized WO_3 nanorods is the [0002] direction (*c*-axis).

Much progress in the synthesis of WO_3 nanowires and nanorods has been achieved by Guo and Yao et al.[15,18] They used lithium salts (Li_2WO_4 and Li_2SO_4) as tungsten source and capping agent. They found that capping agent Li_2SO_4 cannot be replaced by sodium salts; Li^+ ions and SO_4^{2-} ions play an important role in the formation of one-dimensional WO_3 nanostructures. However, in our experiments, we found that the very abundant and economical sodium salts can be used as tungsten source (Na_2WO_4) and capping agent (NaCl) to synthesize high-quality crystalline WO_3 nanorods, which has more advantages in the large-scale production of crystalline WO_3 nanorods. The growth mechanism of the WO_3 nanorods has been proposed in our previous work.[13] In brief, WO_3 nanorods preferentially grow along the *c*-axis with the capping action of NaCl after the decomposition of H_2WO_4 formed by the reaction between H^+ ions and WO_4^{2-} ions in an acidic solution. Different growth rates of crystal planes resulted from the capping action of Na^+ and Cl^- ions, resulting in the preferential growth of WO_3 nanorods along their *c*-axis.[13] From our experimental results, it can be found that a low amount of NaCl realizes a successful selective capping action for some crystal planes. However, excess NaCl has an adverse effect on the formation of uniform nanorods. It is believed that the excess capping agent covered the growth planes of some nanorods, resulting in the formation of irregular nanorods and nanoparticles.

The electrochromic properties of the WO_3 nanorods were measured by a two-electrode electrochemical cell in 0.5 mol/L

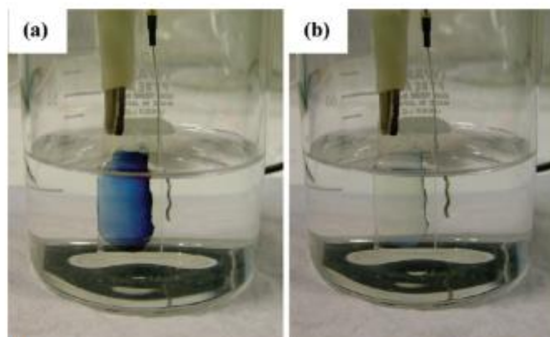

Figure 5. Color changes of the as-prepared electrochromic film between (a) coloration at −1.0 V and (b) bleaching at +1.0 V.

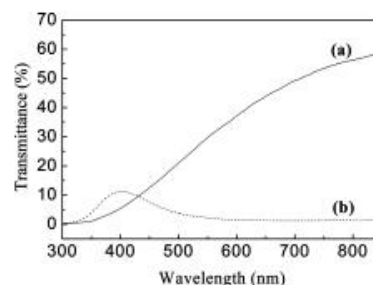

Figure 6. Transmittance spectra of the as-prepared electrochromic film measured at (a) +1.0 V and (b) −1.0 V for 300 s, respectively.

H_2SO_4 aqueous solution. WO_3-nanorod-coated ITO glass and Pt wire were used as working electrode and counter electrode, respectively. The as-prepared electrochromic film is almost colorless before electrochemical experiments. It quickly displayed a deep blue color at −1.0 V and bleached to colorless state at +1.0 V, as shown in Figure 5. The colored electrochromic film can retain its colors for several days after the applied voltages were removed. It is promising that significant energy-saving can be realized using this kind of electrochromic film.

Figure 6 shows the in situ measured transmittance spectra of the electrochromic film measured at +1.0 V and −1.0 V for 300 s, respectively. It can be calculated that the maximum contrast of ~54.9% occurs at the wavelength of ~800 nm. There is a clear transmittance peak at ~400 nm, which indicates that the film can show blue color at a voltage of −1.0 V and it has maximum absorption at a red-end wavelength. Some literatures[9−11] reported the transmittance by using a wavelength of 632.8 nm as the maximum absorbance wavelength of WO_3 electrochromic films. For the purpose of comparison, the in situ coloration/bleaching switching of the as-prepared electrochromic film was measured at 632.8 nm, as shown in Figure 7a. The maximum optical modulation (*T*%) of coloration/bleaching was found to be ~33.9% after applying a ±1.0 V voltage biasing for 300 s, respectively, which corresponds to the transmittance study in Figure 6. The coloration and bleaching times are extracted as the time required for 70% changes in the whole transmittance modulation at 632.8 nm. The coloration time and bleaching time for 70% transmittance changes are found to be 25.2 and 18.0 s, respectively; both of them are faster than that measured in lithium-based electrolyte[13] and comparable to amorphous structures,[9−11] which makes crystalline WO_3 nanorod film suitable for electrochromic devices in acidic electrolytes. This should be attributed to the large active specific surface of the

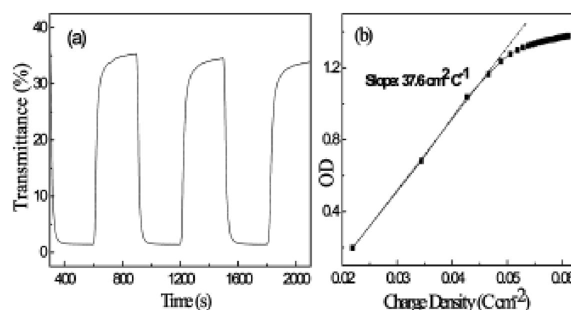

Figure 7. (a) Coloration/bleaching switching response of the electrochromic film measured at +1.0 V and −1.0 V and (b) OD variation with respect to the charge density (measured at 632.8 nm, +1 V bias for 300 s).

crystalline WO_3 nanorods, which facilitated the ion intercalation and deintercalation. The total cathodic charge density is found to be 114.5 mC cm^{-2} mg^{-1} after 300 s of −1 V biasing. The value is much higher than those of the other reported WO_3 electrochromic materials, which usually have values of ~3 mC cm^{-2} mg^{-1} for crystalline, ~9 mC cm^{-2} mg^{-1} for amorphous films,[19] and 32 mC cm^{-2} mg^{-1} for the recently reported crystalline WO_3 nanoparticles.[12] The highly enhanced H^+ ions insertion should be attributed to a large active specific surface area and the special tunnel structure[15] of hexagonal crystalline WO_3 nanostructures.

The coloration efficiency (CE) represents the change in the optical density (OD) per unit charge density (Q/A) during switching and can be calculated according to the formula: CE = $\Delta OD/(Q/A)$, where OD = $\log(T_{bleach})/T_{color})$. Figure 7b shows a plot of OD versus the extracted charge density at +1 V of bleaching potential and at the wavelength of 632.8 nm. The CE was extracted as the slope of the line fitted to the linear region of the curve. The calculated CE value is 37.6 cm^2 C^{-1}. This value is lower than that of the amorphous film reported by Lee et al.,[20] which could probably be attributed to the slower diffusion of H^+ ions in crystalline WO_3 as compared to the amorphous structure. However, this value is comparable to the other reported crystalline nanostructures,[12] such as the mixture of nanospheroids/nanorods and nanoparticles, which have the values of 24 and 42 cm^2 C^{-1}, respectively. Another point to notice: although the charge density continued to increase under the biasing, the OD was almost a constant value after a short time during the voltage switching. In our case, the OD "saturation" corresponding to a slope change in Figure 7b, occurred at 52 mC cm^{-2}. Relating back to Figure 7a, the transmittance of film at this moment was obtained after 42 s of switching, which corresponds to ~87% of the total optical modulation. It implies that the major optical modulation was completed in the short duration during the voltage switching, whereas further biasing only leads to small optical modulation. A similar trend has been observed in the other reported crystalline WO_3 nanostructures.[12,21]

4. Conclusion

Uniform crystalline WO_3 nanorods were synthesized by a facile hydrothermal process with $Na_2WO_4 \cdot 2H_2O$ as the tungsten source and NaCl as the capping agent. Systematic investigations of the influence of precursor pH and the amount of capping agent on the morphologies of the products have been carried out. It was found that uniform crystalline WO_3 nanorods can be synthesized at pH 2.0 with suitable NaCl content. A transparent thin film was successfully prepared by coating the as-synthesized WO_3 nanorods onto the surface of ITO-coated glass. The film shows fast electrochromic switching response, comparable contrast and coloration efficiency, and much higher charge density (114.5 mC cm^{-2} mg^{-1}) than conventional amorphous WO_3 films in 0.5 mol/L H_2SO_4 electrolyte. The fast switching response and high H^+ insertion ability of the as-prepared electrochromic film are attributed to the large active specific surface area of the as-synthesized WO_3 nanorods and the application of acidic electrolyte (H_2SO_4) containing smaller inserted ions (H^+) than Li^+ ions in lithium-based electrolytes. The as-synthesized crystalline WO_3 electrochromic film has potential applications in energy-saving smart windows due to the fast switching response and in capacitors due to the enhanced ion-insertion ability.

References and Notes

(1) Granqvist, C. G. *Handbook of Inorganic Electrochromic Materials*; Elsevier: Amsterdam, Netherlands, 1995.
(2) Santato, C.; Odziemkowski, M.; Ulmann, M.; Auustynski, J. *J. Am. Chem. Soc.* **2001**, *123*, 10639.
(3) Deb, S. K. *Sol. Energy Mater. Sol. Cells* **2008**, *92*, 245.
(4) Baeck, S.-H.; Choi, K.-S.; Jaramillo, T. F.; Stucky, G. D.; McFarland, E. W. *Adv. Mater.* **2003**, *15*, 1269.
(5) Feng, M.; Pan, A. L.; Zhang, H. R.; Li, Z. A.; Liu, F.; Liu, H. W.; Shi, D. X.; Zou, B. S.; Gao, H. J. *Appl. Phys. Lett.* **2005**, *86*, 141901.
(6) Rossinyol, E.; Prim, A.; Pellicer, E.; Arbiol, J.; Hernández-Ramírez, F.; Peiró, F.; Cornet, A.; Morante, J. R.; Solovyov, L. A.; Tian, B.; Bo, T.; Zhao, D. *Adv. Funct. Mater.* **2007**, *17*, 1801.
(7) Niklasson, G. A.; Granqvist, C. G. *J. Mater. Chem.* **2007**, *17*, 127.
(8) Granqvist, C. G. *Sol. Energy Mater. Sol. Cells* **2000**, *60*, 201.
(9) Deepa, M.; Joshi, A. G.; Srivastava, A. K.; Shivaprasad, S. M.; Agnihotry, S. A. *J. Electrochem. Soc.* **2006**, *153*, C365.
(10) Deepa, M.; Saxena, T. K.; Singh, D. P.; Sood, K. N.; Agnihotry, S. A. *Electrochim. Acta* **2006**, *51*, 1974.
(11) Subrahmanyam, A.; Karuppasamy, A. *Sol. Energy Mater. Sol. Cells* **2007**, *91*, 266.
(12) Lee, S.-H.; Deshpande, R.; Parilla, P. A.; Jones, K. M.; To, B.; Mahan, A. H.; Dillon, A. C. *Adv. Mater.* **2006**, *18*, 763.
(13) Wang, J. M.; Khoo, E.; Lee, P. S.; Ma, J. *J. Phys. Chem. C* **2008**, *112*, 14306.
(14) Cao, G. Z. *Nanostructures and Nanomaterials: Synthesis, Properties and Applications*;Imperial College Press: London, 2004.
(15) Gu, Z. J.; Li, H. Q.; Zhai, T. Y.; Yang, W. S.; Xia, Y. Y.; Ma, Y.; Yao, J. N. *J. Solid State Chem.* **2007**, *180*, 98.
(16) Lee, Y.-J.; Sounart, T. L.; Liu, J.; Spoerke, E. D.; McKenzie, B. B.; Hsu, J. W. P.; Voigt, J. A. *Cryst. Growth Des.* **2008**, *8*, 2036.
(17) Yu, S.-H.; Antonietti, M.; Co1lfen, H.; Hartmann, J. *Nano Lett.* **2003**, *3*, 379.
(18) Gu, Z. J.; Ma, Y.; Yang, W. S.; Zhang, G. J.; Yao, J. N. *Chem. Commun.* **2005**, 3597.
(19) Deshpande, R.; Lee, S.-H.; Mahan, A. H.; Parilla, P. A.; Jones, K. M.; Norman, A. G.; To, B.; Blackburn, J. L.; Mitra, S.; Dillon, A. C. *Solid State Ionics* **2007**, *178*, 895.
(20) Lee, S. H.; Cheong, H. M.; Tracy, C. E.; Mascarenhas, A.; Czanderna, A. W.; Deb, S. K. *Appl. Phys. Lett.* **1999**, *75*, 1541.
(21) Deepa, M.; Srivastava, A. K.; Agnihotry, S. A. *Acta Mater.* **2006**, *54*, 4583.

JP901650V

Temperature / voltage calibration curve of the aluminum resistance.

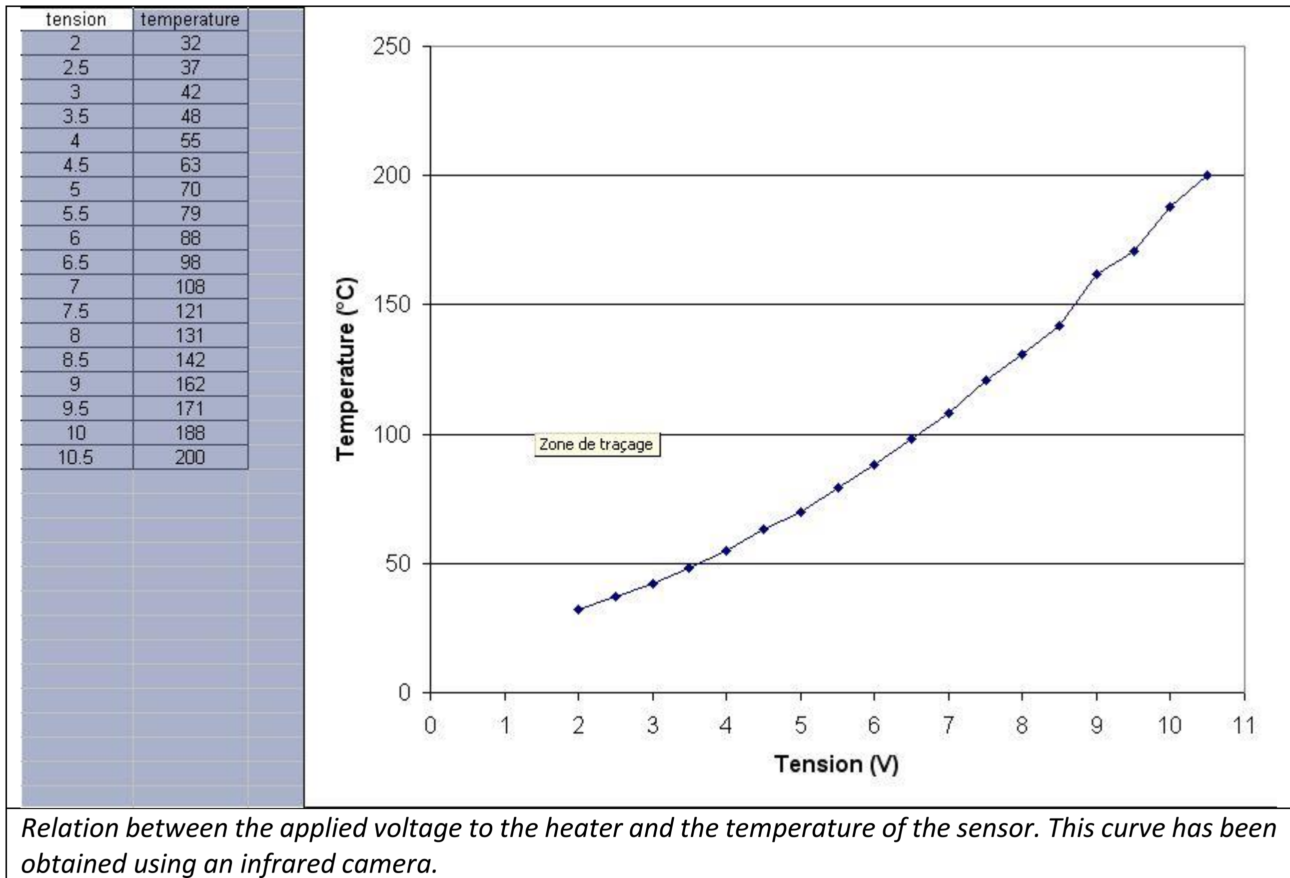

tension	temperature
2	32
2.5	37
3	42
3.5	48
4	55
4.5	63
5	70
5.5	79
6	88
6.5	98
7	108
7.5	121
8	131
8.5	142
9	162
9.5	171
10	188
10.5	200

Relation between the applied voltage to the heater and the temperature of the sensor. This curve has been obtained using an infrared camera.

Protocol characterization of gas sensors (proposal)

Perform a characterization of your sample at the following temperatures: 100°C, 150°C, 200°C, 250°C, 300°C.

For each temperature:

- Create a first file in which you will record what happens when you increase the temperature with no air flow. Wait until the resistance is roughly stabilized.
- Create a second file in which you will record the sensor response to gas. The protocol can be the following:

- apply the voltage during 30s with no air flow
- dry air during 2 min
- ethanol during 2 min
- dry air during 2 min
- ethanol during 2 min
- dry air during 2 min
- NH_3 during 2 min
- dry air during 2 min
- NH_3 during 2 min
- dry air until stabilization

Witness treatment

The witness wafer is initially composed of a superposition of layers represented below:

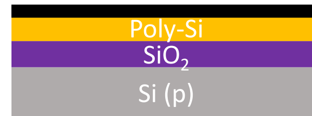

The black layer represents the predeposition oxide.

Step 1 :

- Protect the wafer over 1/4 of its width, then attack the pre-deposition oxide. Deduce its thickness $\mathbf{e_d}$.
- Measure the V/I of poly-Si.

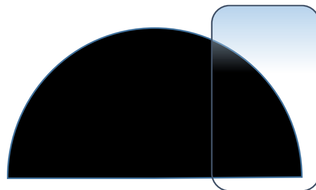

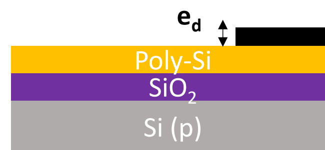

Step 2:

- Protect the wafer over 3/4 of its width, then attack the poly-Si. Deduce its thickness $\mathbf{e_p}$.

- Deduce the resistivity of the poly-Si.

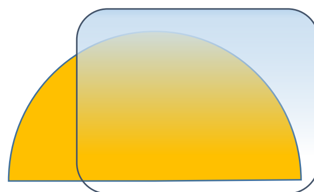

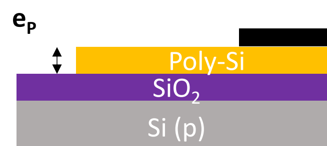

⇒ **Place the witness in the dry oxidation oven**

Step 3 :

- - Protect the wafer over half its width, then attack the dry oxide. Measure its thickness $\mathbf{e_{ox}}$.